Polymer Chemistry

ROYAL SOCIETY OF CHEMISTRY

PAPER

View Article Online
View Journal | View Issue

Check for updates

Cite this: *Polym. Chem.*, 2023, **14**, 3203

Oxygen-free polymers: new materials with low dielectric constant and ultra-low dielectric loss at high frequency†

Jiaren Hou,[a] Jing Sun*[a,b] and Qiang Fang *[a]

Two new oxygen-free polymers (**p-4F-BVS** and **p-6F-BVS**) have been prepared through a thermal crosslinking reaction based on benzocyclobutene-containing monomers that contain only carbon, hydrogen, fluorine, and silicon atoms without oxygen atoms. These polymers display excellent dielectric performance at a high frequency of 10 GHz with dielectric constants (D_k) of 2.42 and 2.58 and dielectric losses (D_f) of 6.4×10^{-4} and 1.1×10^{-3} for **p-6F-BVS** and **p-4F-BVS**. For comparison, a polymer (**p-6F-BCB**) containing oxygen atoms has been synthesized, which exhibits a D_k of 2.48 and a D_f of 2.33×10^{-3}. These results indicate that oxygen atoms have a negative effect on the dielectric loss of the organic materials, while the introduction of the bulky $-CF_3$ groups is positive for decreasing the dielectric constants of the polymers. Such results are significant for the design of low dielectric loss materials. The two polymers also exhibit a low thermal expansion coefficient (CTE) of about 55 ppm $°C^{-1}$ in the range of temperatures from 30 to 300 °C. These data indicate that the two polymers are highly desirable for application as advanced packaging materials in the microelectronics industry.

Received 5th May 2023,
Accepted 16th June 2023

DOI: 10.1039/d3py00494e

rsc.li/polymers

Open Access Article. Published on 20 June 2023. Downloaded on 4/6/2026 2:06:47 PM.
This article is licensed under a Creative Commons Attribution-NonCommercial 3.0 Unported Licence.

Introduction

In recent years, high-frequency communication technology has been widely applied in many fields such as mobile communication, aerospace, artificial intelligence and autopilot.[1–3] To achieve high-quality electronic communication, devices should meet certain requirements including ultra-fast signal transmission speed, extremely low signal delay and multiple user connections, which leads to the miniaturization and densification of electronic devices.[1,2] In many cases, however, resistance–capacitance delay, crosstalk and energy loss during signal transmission usually occur.[4,5] Thus, exploring and developing dielectric materials with a low dielectric constant (D_k) and low dielectric loss (D_f) are necessary.

It is known that the transmission speed (v) and transmission loss (α) of the signal in the dielectrics are closely related to D_k and D_f, as shown in eqn (1) and (2):[4,6]

$$v = kcD_k^{-\frac{1}{2}} \quad (1)$$

$$\alpha = k'fD_k^{\frac{1}{2}}D_f \quad (2)$$

where c is the speed of light, f is the frequency, and k and k' are constants. Obviously, v is dependent on D_k and α is closely related to D_f. Therefore, to improve the transmission speed and quality of the signal, the reduction of D_k and D_f is necessary. Usually, it is desirable for dielectric materials to have a D_k below 2.5 and a D_f lower than 0.001 at high frequencies above 5 GHz, while few low-k materials exhibit such low D_k and low D_f.

In principle, the D_k of organic materials can be effectively reduced through two main approaches.[7] The first one is to reduce the polarizability of the molecules *via* introducing low polarizable groups into the backbone or side chains of the molecules, such as C–F, Si–C, and C–C groups. The second one is to lower the dipole density through attaching bulky groups to the polymers and using pore-creating technology.[8] Although many attempts have been made to reduce the D_k of the polymers, including adding fluorinated groups and incorporating bulk adamantine[9] or spiro-type aryl groups[10] into the polymers, few investigations on the reduction of the D_f have been reported in the past decades. The reason may be that

[a]*Key Laboratory of Synthetic and Self-Assembly Chemistry for Organic Functional Molecules, Center for Excellence in Molecular Synthesis, Shanghai Institute of Organic Chemistry, University of Chinese Academy of Sciences, Chinese Academy of Sciences, 345 Lingling Road, Shanghai 200032, P. R. China.*
E-mail: qiangfang@sioc.ac.cn, sunjing@sioc.ac.cn
[b]*CAS Key Laboratory of Energy Regulation Materials Shanghai Institute of Organic Chemistry, 345 Lingling Road, Shanghai 200032, P. R. China*

†Electronic supplementary information (ESI) available: Characterization of compounds **4F-BVS** and **6F-BVS**, determination of crosslinking density (PDF). See DOI: https://doi.org/10.1039/d3py00494e

Open Access Article. Published on 20 June 2023. Downloaded on 4/6/2026 2:06:47 PM.
This article is licensed under a Creative Commons Attribution-NonCommercial 3.0 Unported Licence.

there are many complicated factors that affect the D_f including polarization characteristics and molecular stacking. A study from Li's group indicates that polyimides with phenyl sulfide groups exhibit reduced D_f when the content of phenyl sulfide increases because the high content may affect the degree of micro-crystallinity.[11]

Moreover, for practical applications, low-*k* materials must possess certain characteristics including high thermostability, ease of processing, high hydrophobicity and good film-forming ability.[12] Hence, it is of significance to explore new methods to achieve low-*k* materials with outstanding comprehensive properties. We have therefore designed and synthesized two intrinsic low-*k* polymers with ultra-low D_f based on monomers with fluorinated and thermo-crosslinkable benzocyclobutene (BCB) groups without oxygen atoms (**4F-BVS** and **6F-BVS**, shown in Fig. 1). The cured **4F-BVS** and **6F-BVS** exhibit D_k values of 2.42 and 2.57, respectively, as well as D_f values of 6.4×10^{-4} and 1.1×10^{-3}, respectively, at a frequency of 10 GHz. For comparison, a monomer containing oxygen atoms (**6F-BCB**, Fig. 1) has been prepared, and the cured **6F-BCB** (**p-6F-BCB**) exhibits a D_k of 2.48 and a D_f of 2.33×10^{-3}. These data indicate that the oxygen-free feature of the polymers has a positive effect on the D_f of the polymers, while introducing the bulky CF_3 groups can decrease the D_k of the polymers. Moreover, enhancing the cross-linking density can be beneficial for lowering the D_f of the polymers. The thermal expansion coefficient (CTE) is an important parameter for the application of the materials; thus the CTE data of the two polymers have also been investigated, exhibiting a CTE of about 55 ppm $°C^{-1}$ within the temperature range 30–300 °C. Such excellent properties of the two polymers imply that the polymers are suitable as interlayer dielectric resins or advanced packaging materials for applications in the microelectronics industry. Here, we report the details.

Experimental section

Materials

Dichloromethylvinylsilane, *N,N,N′,N′*-tetramethylethylenediamine (TMEDA), 1,2,4,5-tetrafluorobenzene, and 1,4-bis(trifluoromethyl)benzene were purchased from TCI (Shanghai) Development Co. 4-Bromobenzocyclobutene, *N*-bromosuccinimide (NBS) and *n*-butyl lithium (*n*-BuLi) were purchased from Chemtarget Technologies Co., Innocent (Beijing) Technology Co. and Adamas Reagent Co., respectively. THF was treated using a solvent handling system before use. All solvents were used as received unless stated otherwise.

Method

^{1}H NMR, ^{13}C NMR, and ^{19}F NMR spectra were recorded on an AVANCE 500 spectrometer with $CDCl_3$ as the solvent. Elemental analysis (EA) was carried out using an Elementar VARIO ELIII apparatus. High-resolution mass spectrometry (HRMS) was acquired using an Agilent technologies 6230 TOF LC/MS instrument. Fourier transform-infrared (FT-IR) spectra were measured *via* a Thermo Scientific Nicolet spectrometer with KBr pellets in air. Differential scanning calorimetry (DSC) curves were obtained with a TA instrument (DSC Q200) at a heating rate of 10 °C min^{-1} under a nitrogen flow. Thermogravimetric analysis (TGA) curves were monitored on a TG 209F1 apparatus in nitrogen with a heating rate of 10 °C min^{-1}. Dynamic mechanical analysis (DMA) was carried out on a DMA Q800 instrument in nitrogen with a heating rate of 5 °C min^{-1}. Thermal mechanical analysis (TMA) was performed on a TA Q400 instrument in nitrogen with a heating rate of 5 °C min^{-1}. D_k and D_f were measured using a Keysight *n*5227A vector network analyzer with a split post-dielectric resonator at a frequency of 10 GHz. X-ray diffraction (XRD) was performed on a PANalytical X'Pert Powder instrument.

Preparation of BVCS

BVCS (see Scheme 1) was synthesized according to a previously reported route.[13] The general procedure is as follows: 4-bromobenzocyclobutene (10.0 g, 54.63 mmol) was added dropwise to a stirring solution of anhydrous THF (20 mL) containing dichloromethylvinylsilane (9.3 g, 65.56 mmol), magnesium turnings (1.4 g, 57.56 mmol) and a grain of iodine at room

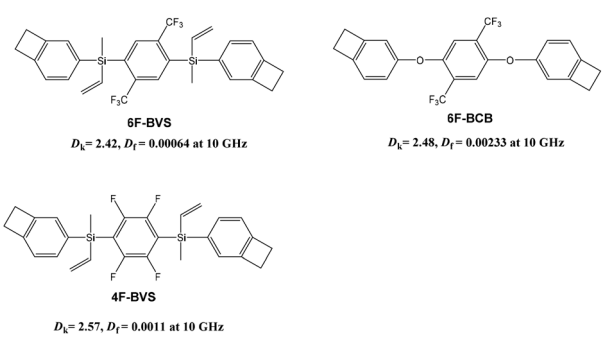

Fig. 1 Dielectric properties of the polymers based on the BCB monomers with and without oxygen atoms.

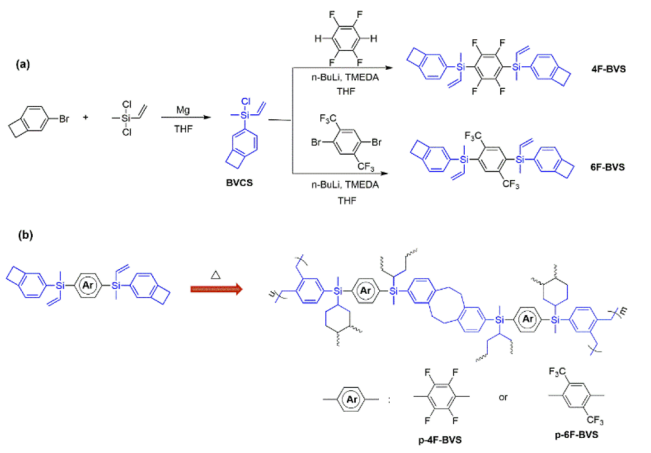

Scheme 1 The procedure for the synthesis of monomers (a) and polymers (b).

This journal is © The Royal Society of Chemistry 2023

Open Access Article. Published on 20 June 2023. Downloaded on 4/6/2026 2:06:47 PM.
This article is licensed under a Creative Commons Attribution-NonCommercial 3.0 Unported Licence.

temperature under a nitrogen atmosphere. After being stirred at room temperature for an additional 6 h, the mixture was poured into 200 mL of *n*-hexane and filtered to remove the precipitate. The filtrate was concentrated under reduced pressure. The obtained residue was subjected to distillation to give **BVCS** in a yield of 79% as a colorless transparent liquid.

Preparation of 4F-BVS

A solution of *n*-BuLi in hexane (14 mL, 2.5 M) was slowly added *via* a syringe into a solution of TMEDA (4.1 g, 35.18 mmol) in anhydrous THF (20 mL) at −78 °C under N_2 during a period of 30 min. 1,2,4,5-Tetrafluorobenzene (2.4 g, 15.99 mmol) was then added dropwise to the mixture with stirring. After being maintained at the temperature for an additional 1 h, the mixture was added to a solution of **BVCS** (7.0 g, 33.53 mmol) in THF (20 mL) using a syringe, warmed to room temperature naturally and stirred at room temperature for 4 h. The reaction mixture was quenched with ethanol and concentrated under reduced pressure. The obtained residue was diluted with ethyl acetate (200 mL). The obtained solution was washed with brine (1 × 100 mL) and water (3 × 200 mL), dried over anhydrous Na_2SO_4, filtered, and concentrated to give the crude product. The pure **4F-BVS** was obtained as a white solid in a yield of 51% after treating the crude product with flash chromatography using petroleum (60–90 °C) as the eluent. ^{1}H NMR (500 MHz, $CDCl_3$): δ 7.43 (d, J = 7.2 Hz, 2H), 7.27 (s, 2H), 7.10 (d, J = 7.2 Hz, 2H), 6.63 (dd, J = 20.3, 14.6 Hz, 2H), 6.23 (dd, J = 14.6, 3.2 Hz, 2H), 5.90 (dd, J = 20.3, 3.2 Hz, 2H), 3.21 (s, 8H), 0.78 (s, 6 H). ^{13}C NMR (126 MHz, $CDCl_3$): δ 149.68, 149.70, 148.21, 147.78, 145.84, 134.95, 134.60, 132.61, 132.42, 127.94, 122.25, 116.99, 29.97, 29.93, −3.24. ^{19}F NMR (376 MHz, $CDCl_3$): δ −126.34. HRMS (m/z): calcd for $[M + NH_4]^+$: 512.1847. Found: 512.1843. Elemental analysis: calcd for $C_{28}H_{26}F_4Si_2$, C, 67.99; H, 5.30; F, 15.36. Found, C, 67.75; H, 5.49; F, 15.50.

Preparation of 6F-BVS

By using a similar route to that used for the synthesis of **4F-BVS**, **6F-BVS** was synthesized in a yield of 69% as a white solid. ^{1}H NMR (500 MHz, $CDCl_3$): δ 8.02 (s, 2H), 7.29 (d, J = 7.2 Hz, 2H), 7.13 (s, 2H), 7.06 (d, J = 7.2 Hz, 2H), 6.51 (dd, J = 20.3, 14.6 Hz, 2H), 6.22 (dd, J = 14.6, 3.3 Hz, 2 H), 5.80 (dd, J = 20.3, 3.3 Hz, 2H), 3.19 (s, 8H), 0.73 (s, 6H). ^{13}C NMR (126 MHz, $CDCl_3$): δ 147.78, 145.65, 137.69, 135.57, 135.37, 135.11, 133.03, 132.92, 131.98, 128.19, 127.38, 122.04, 29.93, 29.87, −3.20. ^{19}F NMR (376 MHz, $CDCl_3$) δ −57.95; HRMS (m/z): calcd for $[M + NH_4]^+$: 576.1972. Found: 576.1971. Elemental analysis: calcd for $C_{30}H_{28}F_6Si_2$, C, 64.49; H, 5.05; F, 20.40. Found, C, 64.83; H, 5.13; F, 20.48.

Curing of the monomers

A monomer (about 1.2 g) in a flat-bottomed glass mold (cylinder- or cuboid-shape) was placed into a quartz tube furnace, and the furnace was heated under reduced pressure to 100 °C and maintained at that temperature for 1 h until the monomer had fully melted and no bubble from the melting monomer was observed. The reduced pressure was released, and nitrogen was introduced into the furnace. The furnace was then heated at 200 °C for 1 h, 220 °C for 1 h, 240 °C for 2 h and 260 °C for 1 h, respectively. Thus, a fully cured sample was obtained. The size and shape of the samples varied according to the testing requirements. For the CTE test, a cylinder-shaped sample was needed, and it was prepared in a mold with a diameter of 10 mm and a height of 2 mm. For the DMA test, a cuboid-shaped sample was needed, and it was prepared in a mold with a length of 30 mm, a width of 10 mm and a height of 2 mm. For the measurement of dielectric properties and water uptake, a cylinder-shaped sample was needed, and it was prepared in a mold with a diameter of 30 mm and a height of 0.8 mm.

Results and discussion

Preparation and characterization of monomers

The fluorinated benzocyclobutene monomers **4F-BVS** and **6F-BVS** were prepared by a two-step reaction. Firstly, the intermediate **BVCS** was synthesized by a nucleophilic substitution reaction between dichloromethylvinylsilane and bromobenzocyclobutene. Next, the intermediate **BVCS** further reacted with fluoro-containing compounds in the presence of *n*-BuLi and the organic amine TMEDA (Scheme 1a) to give **4F-BVS** and **6F-BVS**. These two monomers exhibit good solubility in common organic solvents and have a low melting point of below 90 °C, suggesting the good processability of the monomers.

The chemical structures of **4F-BVS** and **6F-BVS** were characterized by ^{1}H NMR, ^{13}C NMR, ^{19}F NMR, FI-IR, HRMS and elemental analysis (EA), and the ^{1}H NMR spectra of **4F-BVS** and **6F-BVS** are depicted in Fig. 2. As shown in Fig. 2, the peak at 0.78 ppm is attributed to the protons in Si–CH_3, while the peak at 3.21 ppm belongs to the protons of –CH_2–CH_2– in the four-membered ring of benzocyclobutene. In addition, the peaks at 5.88 ppm, 6.21 ppm and 6.59 ppm are assigned to the protons in –CH=CH_2 connected to the Si atom. In Fig. 2b, the peak at 8.02 ppm belongs to the aromatic protons of the tetra-substituted benzene in **6F-BVS**. In the ^{13}C NMR spectra (see the ESI, Fig. S2 and S5†), the signals for the carbon atoms in

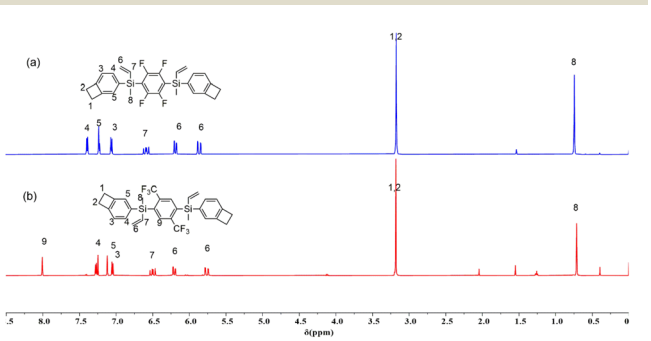

Fig. 2 ^{1}H NMR spectra of **4F-BVS** (a) and **6F-BVS** (b).

Open Access Article. Published on 20 June 2023. Downloaded on 4/6/2026 2:06:47 PM.
This article is licensed under a Creative Commons Attribution-NonCommercial 3.0 Unported Licence.

the four-membered ring of the BCB group appear at 29.93 ppm and 29.97 ppm. In the ^{19}F NMR (see the ESI, Fig. S3 and S6†), the characteristic peaks of the fluorine atoms in **4F-BVS** and **6F-BVS** appear at −126.33 and −57.96 ppm, respectively. Based on the data depicted in the ESI† and the data shown in Fig. 2, it is obvious that all the data are consistent with the proposed structures.

Curing behaviour of the monomers

It is well known that the BCB group can be easily converted to an *o*-quinodimethane or a diradical intermediate at high temperatures. This intermediate has a tendency to form an eight-membered ring or undergo a self-polymerization reaction. In particular, this intermediate is able to react with double bonds *via* the Diels–Alder reaction to form six-membered rings.[14,15] To well understand the curing process of **4F-BVS** and **6F-BVS**, a schematic mechanism is described in Scheme 1b.

The curing behavior was monitored by DSC, and the results are depicted in Fig. 3, As shown in Fig. 3, **4F-BVS** and **6F-BVS** display melting points of about 80 °C and an exothermic reaction occurs around 225 °C, indicating a wide processing window. The two monomers show the maximum exothermic peak at 259 °C, which is ascribed to the ring-opening reaction and thermal polymerization of BCB groups. This phenomenon is in accordance with the curing process of the reported BCB resins.[16,17] In addition, no exothermic peak appears in the second scan, indicating that the monomers have cured completely. The curing degree of the monomers was characterized by FI-IR (Fig. 4). As can be seen from Fig. 4, in the cured monomers, the absorption peaks at 2919 cm^{-1} and 1465 cm^{-1} attributed to methylene in BCB[18] disappear, and the characteristic absorptions at 3059 cm^{-1} and 1642 cm^{-1} assigned to the =CH and C=C stretching vibrations disappear. The peak at 962 cm^{-1} attributed to the C–H bending vibration in vinyl groups is also significantly reduced. In the FI-IR spectra of the cured polymers, a peak of ring-opening products appears at 1493 cm^{-1}. These results indicate that **4F-BVS** and **6F-BVS** have been converted to the cross-linked polymers **p-4F-BVS** and **p-6F-BVS**.

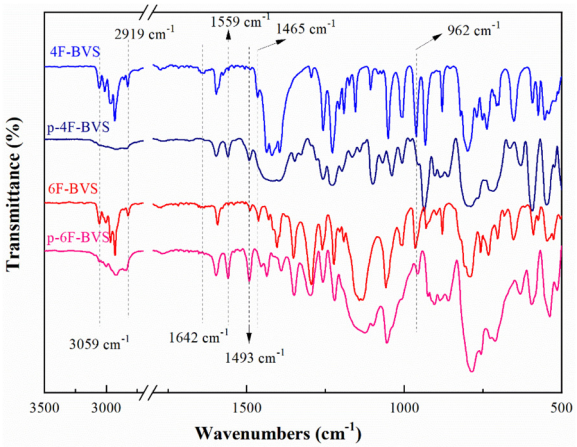

Fig. 4 FI-IR spectra of **4F-BVS** and **6F-BVS** before and after curing.

Thermostability

High thermostability is an essential feature of the low-*k* materials used in the microelectronics industry. Usually, low-*k* materials are required to endure temperatures of over 400 °C for the fabrication of microelectronics devices.[12] Thus, the thermostability of the polymers **p-4F-BVS** and **p-6F-BVS** was investigated in detail. First, the thermal degradation temperatures of **p-4F-BVS** and **p-6F-BVS** under a nitrogen environment were evaluated by thermogravimetric analysis (TGA). As shown in Fig. 5, the 5% weight loss temperatures (T_{5d}) of **p-4F-BVS** and **p-6F-BVS** are 446 °C and 441 °C, respectively. Meanwhile, the temperatures of the maximum rate of degradation (T_{peak}) are both around 470 °C. The high T_{5d} and T_{peak} values indicate the good heat resistance of the polymers.

The thermomechanical properties of the polymers were further explored by dynamic mechanical analysis (DMA), and the storage modulus and tan δ curves are depicted in Fig. 6. **p-4F-BVS** and **p-6F-BVS** show storage moduli of 2.0 GPa and 1.6 GPa at room temperature, respectively. The storage moduli of the polymers remain stable even when the temperatures

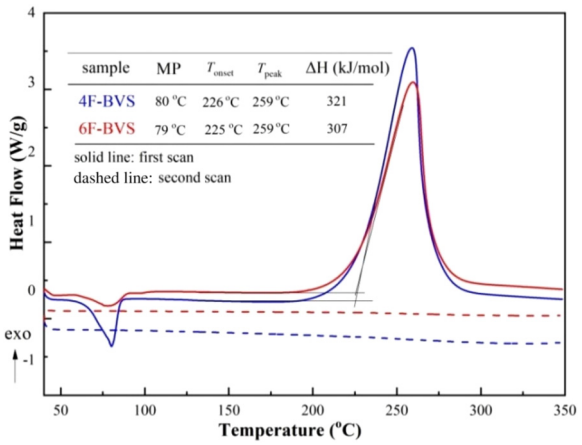

Fig. 3 DSC traces of **4F-BVS** and **6F-BVS**.

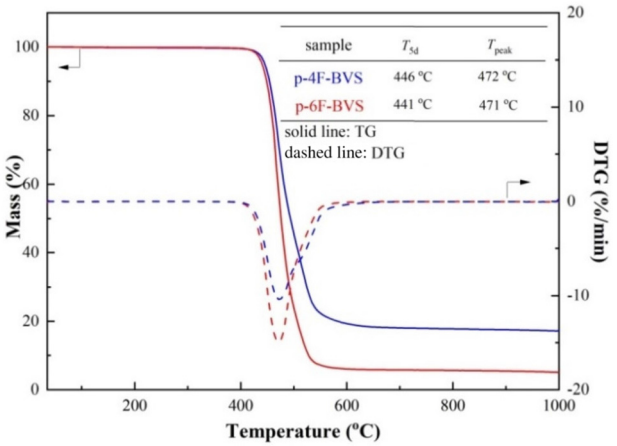

Fig. 5 TGA and DTG curves of **p-4F-BVS** and **p-6F-BVS**.

This journal is © The Royal Society of Chemistry 2023

Open Access Article. Published on 20 June 2023. Downloaded on 4/6/2026 2:06:47 PM.
This article is licensed under a Creative Commons Attribution-NonCommercial 3.0 Unported Licence.

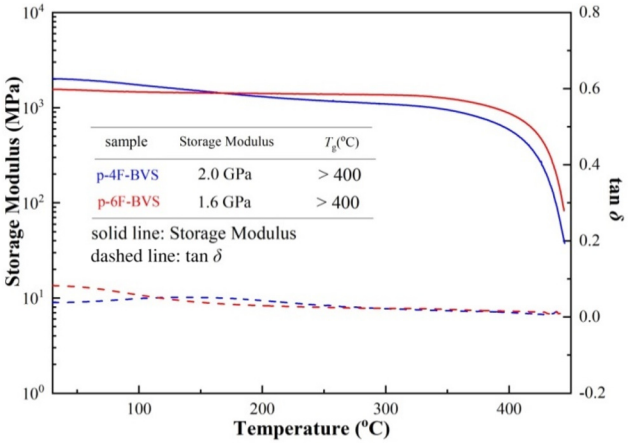

Fig. 6 DMA curves of **p-4F-BVS** and **p-6F-BVS**.

reach over 350 °C. Moreover, no obvious relaxations can be observed in the tan δ curves at test temperatures ranging from 30 °C to 440 °C, illustrating that the T_g values of **p-4F-BVS** and **p-6F-BVS** exceed 400 °C. The T_g values of the two polymers are higher than those of many previously reported BCB resins[19–22] and comparable to those of commercial low-k polymers, such as polyimides,[23,24] SILK resins,[25] and cyanate esters.[26] The reason why the two polymers have high storage moduli and T_g values may be their high cross-linking and rigid structures.

Thermally dimensional stability is one of the important parameters for the evaluation of dielectric polymers, which is closely related to the reliability of microelectronics devices. Therefore, the thermal dimensional stability of **p-4F-BVS** and **p-6F-BVS** was detected by thermal mechanical analysis (TMA). The linear coefficients of thermal expansion (CTEs) of the polymers were calculated based on the results of TMA (Fig. 7). As can be seen from Fig. 7, the CTEs of **p-4F-BVS** and **p-6F-BVS** are 48.10 ppm °C^{-1} and 53.26 ppm °C^{-1} in the range 30–300 °C, respectively, which are lower than that of a commercial BCB-based siloxy-containing resin **DVS-BCB**, 65.0 ppm °C^{-1}.[14] In addition, the CTE of **p-6F-BVS** is slightly

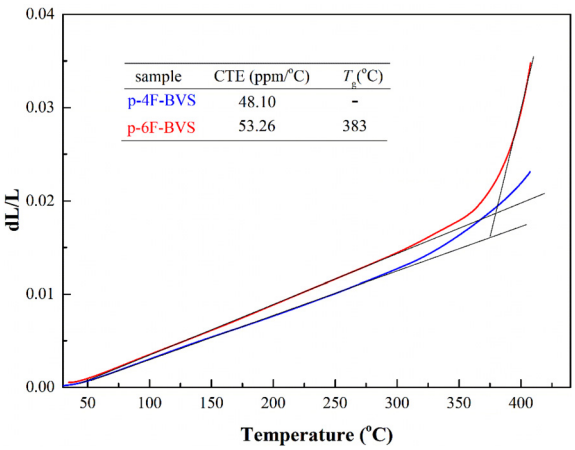

Fig. 7 TMA curves of **p-4F-BVS** and **p-6F-BVS**.

higher than that of **p-4F-BVS**, attributed to the loose stacking caused by the large free volume of the trifluoromethyl groups.

Obviously, the above-mentioned data indicate that **p-4F-BVS** and **p-6F-BVS** possess high thermostability because of their dense cross-linking networks and rigid aromatic backbones.

Hydrophobicity

Good hydrophobicity and low water uptake are necessary for low-k materials because moisture has a great effect on the dielectric performance of the devices during practical application.[12] In order to evaluate the water uptake of the two polymers, a test has been conducted, and the results indicate that **p-4F-BVS** and **p-6F-BVS** exhibit water uptakes of 0.33% and 0.17%, respectively, after being immersed in boiling water for 24 h, as shown in Fig. 8a. Such data are lower than those of the non-fluorinated BCB resins previously reported,[27] indicating that the introduction of fluoro-containing groups can decrease the water uptake of the materials. The contact angles of water on the surface of **p-4F-BVS** and **p-6F-BVS** films were investigated, and the results are depicted in Fig. 8b and c. It can be seen that the polymers display contact angles higher than 96°, suggesting their good surface hydrophobicity.[28,29] Thus, good surface hydrophobicity can prevent water from penetrating into the polymers and endow the polymers with desirable water repellency, contributing to achieving low water uptake. These results imply that the two polymers are suitable for use as protecting materials against moisture.

Dielectric properties

By using the resonance method, the D_k and D_f of the two polymers and the controlling polymer (**6F-BCB**) were measured at a high frequency of 10 GHz, and the results are summarized in Table 1. As can be seen from Table 1, both the polymers exhibit low D_k and D_f at a frequency of 10 GHz. Among the two polymers, **p-6F-BVS** shows a D_k of 2.42 and an ultra-low D_f of 6.4×10^{-4} at 10 GHz, which are lower than those of **p-4F-BVS** and much lower than those of the controlling polymer **p-6F-BCB** with a D_k of 2.48 and a D_f of 2.3×10^{-3}. To the best of our knowledge, few intrinsic materials with a D_k of lower than 2.5 and a D_f of less than 1.0×10^{-3} at high frequencies have been reported. In order to understand how **p-6F-BVS** achieves such low D_k and D_f, the influence of the polymer structure on

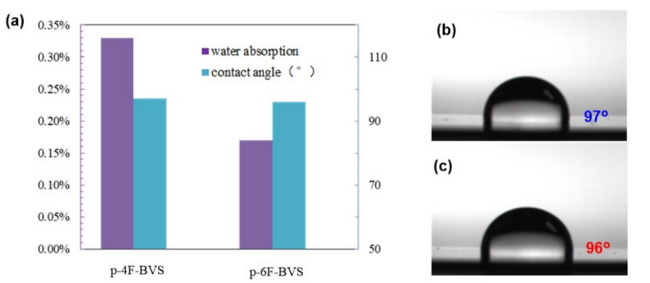

Fig. 8 Hydrophobicity of polymers: (a) column diagram of water absorption and contact angle; (b) contact angles of water on the surfaces of the polymer films: **p-4F-BVS** (b) and **p-6F-BVS**(c).

Open Access Article. Published on 20 June 2023. Downloaded on 4/6/2026 2:06:47 PM.
This article is licensed under a Creative Commons Attribution-NonCommercial 3.0 Unported Licence.

Table 1 Properties of organosilicon-based PFCB resins

Polymers	F_c [a]	D_k	D_f
p-4F-BVS	15.4%	2.57	1.1×10^{-3}
p-6F-BVS	20.4%	2.42	6.4×10^{-4}
p-6F-BCB	25.3%	2.48	2.3×10^{-3}

[a] Fluoro-content of the polymer.

the dielectric properties has been investigated. According to the Debye equation (eqn (3)),

$$\frac{D_k - 1}{D_k + 2} = \frac{4\pi}{3} N\left(\alpha_e + \alpha_d + \frac{\mu^2}{3\kappa_B T}\right) \quad (3)$$

where D_k is the dielectric constant, N is the number density of dipoles, α_e is the electric polarization, α_d is the distortion polarization, and $\mu^2/3\kappa_B T$ is the orientation polarization related to the thermal averaging of permanent electric dipole moments. In comparison with the controlling polymer **p-6F-BCB** based on **6F-BCB** (Fig. 1), **p-6F-BVS** exhibits lower D_k, and the reason may be attributed to the existence of the C–F and Si–C bonds with low polarizability in **p-6F-BVS**. In addition, oxygen-containing groups generally have high molar polarizability,[6] so eliminating oxygen atoms in polymers can reduce the polarizability, resulting in a decrease in α_e.

Relative to **p-4F-BVS**, **p-6F-BVS** also shows lower D_k. The reason is that bulky trifluoromethyl groups can increase the free volume, which is beneficial for reducing dipole density, leading to a decrease in N. Usually, bulky groups can limit the packing of molecular chains, thereby increasing the free volume. In order to verify the proposed assumption, X-ray diffraction (XRD) was employed to measure the distance between molecular chains in the polymers. As can be seen from Fig. 9, all polymers are amorphous, and the diffraction peaks (2θ) of **p-4F-BVS** and **p-6F-BVS** are 14.0° and 12.2°, respectively. According to the Bragg equation, the distances between molecular chains are 0.63 nm and 0.72 nm, respectively. These data illustrate that the bulky group in **p-6F-BVS** can increase the distance between molecular chains, resulting in enhanced free volume. Subsequently, the densities of **p-4F-BVS** and **p-6F-BVS** were measured as 1.200 g cm^{-3} and 1.187 g cm^{-3}, respectively. The lower intrinsic density of **p-6F-BVS** further confirms that the incorporation of the –CF_3 group into the polymer can restrict the accumulation of molecular chains, leading to a decrease in polymer density. In addition, the diffraction peak (2θ) of **p-6F-BCB** is 17.5°, and the corresponding distance between molecular chains is calculated as 0.51 nm. Relative to **p-6F-BVS**, **p-6F-BCB** without the –Si–C═C– unit shows a closer stacking between molecular chains, resulting in a higher intrinsic density of 1.303 g cm^{-3}.

Theoretically, the D_f is mainly related to the polarization and movement of dipoles of polymers within the frequency range of radio waves.[4] In this work, **p-4F-BVS**, **p-6F-BVS**, and **p-6F-BCB** have similar structures, and their dipole movements may be affected by the crosslinking density. The crosslinking density of the polymer is determined by the swelling method in xylene. The crosslinking density parameter (γ) can be calculated from eqn (4):[30,31]

$$\gamma = -\frac{\ln(1-\varphi_r) + \varphi_r + \varphi_r^2}{V_0\left(\frac{\varphi_r^{\frac{1}{3}} - \varphi_r}{2}\right)} \quad (4)$$

$$\varphi_r = \frac{\frac{m_0}{\rho_0}}{\frac{m_0}{\rho_0} + \frac{(m_1 - m_0)}{\rho_c}} \quad (5)$$

Table 2 Crosslinking density parameters (γ) of BCB polymers

Resins	ρ_0 [a] (g cm^{-3})	φ_r	χ	$\gamma \times 10^{-2}$ (mol cm^{-3})
p-4F-BVS	1.200	0.9984	1.50	6.67
p-6F-BVS	1.187	0.9988	0.76	8.14
p-6F-BCB	1.303	0.9980	1.74	5.71

[a] The densities of polymers (ρ_0) were calculated using the following formula: $\rho = m/v$.

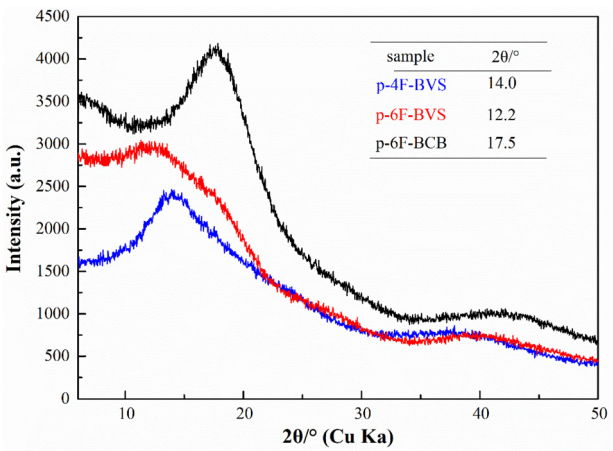

Fig. 9 Powder X-ray diffraction patterns of the polymers.

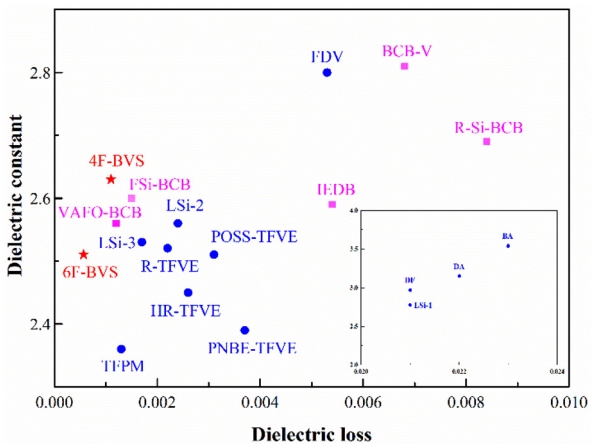

Fig. 10 A comparison of the dielectric constants of **p-4F-BVS** and **p-6F-BVS** with those of the low-*k* resins previously reported at a high frequency of above 5 GHz.

This journal is © The Royal Society of Chemistry 2023

Open Access Article. Published on 20 June 2023. Downloaded on 4/6/2026 2:06:47 PM.
This article is licensed under a Creative Commons Attribution-NonCommercial 3.0 Unported Licence.

Table 3 D_k and D_f of low-k materials at a high frequency of above 5 GHz reported in the literature

Resins	Structure of precursors	D_k	D_f	Ref.
6F-BVS	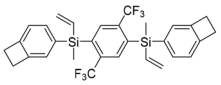	2.51	**0.00057**	This work
4F-BVS	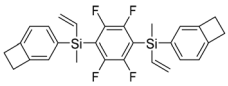	2.63	0.0011	This work
BCB-V	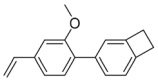	2.81	0.0068	27
R-Si-BCB	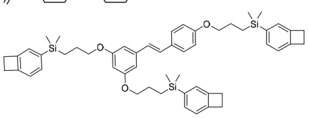	2.69	0.0084	32
DBAF-B	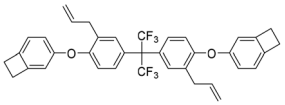	2.56	0.0012	22
FSi-BCB	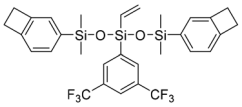	2.60	0.0015	33
IEDB	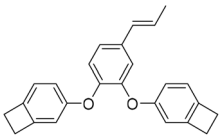	2.59	0.0054	19
IEFB	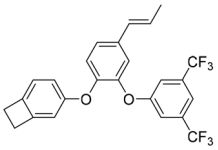	2.56	0.0012	19
PNBE-TFVE	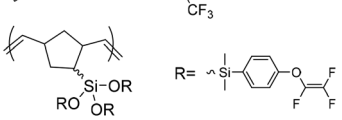	2.39	0.0037	34
R-TFVE	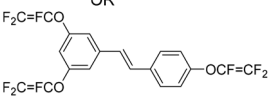	2.52	0.0022	35
HR-TFVE	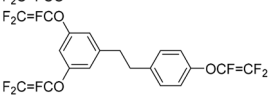	2.45	0.0026	35
TFPM	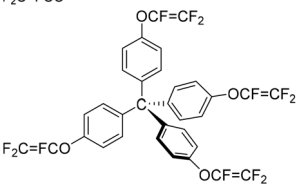	2.36	0.0013	36
POSS-TFVE	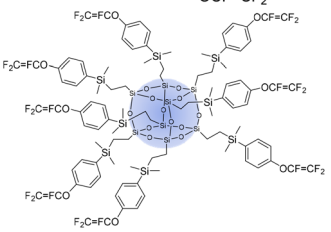	2.51	0.0031	37
FDV	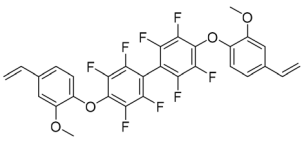	2.80	0.0053	38

Open Access Article. Published on 20 June 2023. Downloaded on 4/6/2026 2:06:47 PM.
This article is licensed under a Creative Commons Attribution-NonCommercial 3.0 Unported Licence.

Table 3 *(Contd.)*

Resins	Structure of precursors	D_k	D_f	Ref.
LSi-1	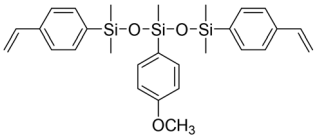	2.78	0.021	39
LSi-2	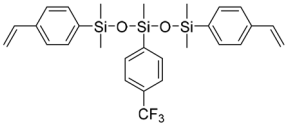	2.56	0.0024	39
LSi-3	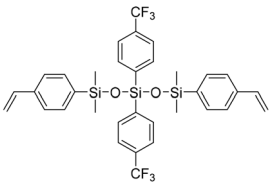	2.53	0.0017	39
BA	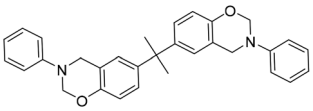	3.54	0.023	40
DA	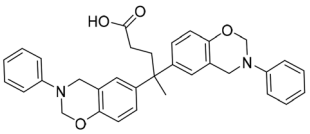	3.15	0.022	40
DF	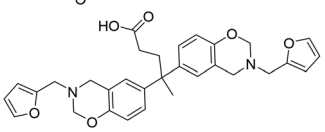	2.97	0.021	40

where φ_r is the equilibrium volume fraction calculated according to eqn (5) by measuring the mass of polymers before swelling in xylene (m_0) and the mass of polymers after swelling to equilibrium (m_1), χ is the BCB polymer–xylene interaction parameter (the calculation of χ is described in the ESI†), V_s is the molar volume of xylene (121.9 cm^3 mol^{-1}), ρ_c is the density of BCB polymers, and ρ_0 is the density of xylene (0.86 g cm^{-3}). The results are listed in Table 2, showing that **p-6F-BVS**, **p-4F-BVS** and **p-6F-BCB** have crosslinking densities of 8.14 × 10^{-2} mol cm^{-3}, 6.67 × 10^{-2} mol cm^{-3} and 5.71 × 10^{-2} mol cm^{-3}, respectively. The gel fractions of the polymers are calculated, which are all close to 1.0 (see Table S1 in the ESI†), indicating that almost all monomers participate in the crosslinking reaction. Compared to **p-6F-BCB**, **p-6F-BVS** has a much higher crosslinking density, consequently showing a lower D_f. This can be attributed to the fact that a higher cross-linking degree can restrict the orientation of units of the polymer in an external electric field.

The dielectric properties of **p-6F-BVS** were comparable to those of the high-frequency low-*k* materials reported recently, which are summarized in Fig. 10 and Table 3.[27,32–40] At a high frequency of 10 GHz, **p-6F-BVS** displays excellent dielectric performance with low D_k and ultra-low D_f, suggesting that it is a suitable candidate as an advanced packaging material for applications in the microelectronics industry.

Conclusion

In summary, two oxygen-free BCB-based monomers **4F-BVS** and **6F-BVS** have been successfully synthesized by a facile route. After thermos-crosslinking, they converted into crosslinked resins (**p-4F-BVS** and **p-6F-BVS**). Both resins exhibit high thermostability, good dielectric properties and good hydrophobicity. Among the two resins, **p-6F-BVS** exhibits better comprehensive properties including a low CTE of 53 ppm $°C^{-1}$ and a low water absorption of 0.17% after immersing in boiling water for 24 h. In particular, **p-6F-BVS** displays a D_k of 2.42 and an ultralow D_f of 6.4 × 10^{-4} at a high frequency of 10 GHz, indicating its excellent dielectric properties. These data based on the two polymers indicate that the materials we prepared have potential applications as low-*k* materials in the field of high-frequency communication. Meanwhile, on the basis of the investigation on the relationship between chemical structure and properties of the materials, this contribution can provide an inspiration to develop new low D_f materials.

Author contributions

Jiaren Hou: synthesis, investigation, data collection, and writing – original draft. Jing Sun: supervision and writing –

 This journal is © The Royal Society of Chemistry 2023

Open Access Article. Published on 20 June 2023. Downloaded on 4/6/2026 2:06:47 PM. This article is licensed under a Creative Commons Attribution-NonCommercial 3.0 Unported Licence.

review & editing. Qiang Fang: supervision, conceptualization, and writing – review & editing.

Conflicts of interest

There are no conflicts to declare.

Acknowledgements

This work was supported by the Natural Science Foundation of China (NSFC, No. 22175195, 22075311 and 21975278) and the Science and Technology Commission of Shanghai Municipality (23ZR1476200).

References

1 J. G. Andrews, S. Buzzi, W. Choi, S. V. Hanly, A. Lozano, A. C. K. Soong and J. C. Zhang, What will 5 g be?, *IEEE J. Sel. Areas Commun.*, 2014, **32**, 1065–1082.
2 B. Bertenyi, 5G evolution: What's next?, *IEEE Wirel. Commun.*, 2021, **28**, 4–8.
3 H. Shi, X. Liu and Y. Lou, Materials and micro drilling of high frequency and high speed printed circuit board: A review, *Int. J. Adv. Des. Manuf. Technol.*, 2018, **100**, 827–841.
4 L. Wang, J. Yang, W. Cheng, J. Zou and D. Zhao, Progress on polymer composites with low dielectric constant and low dielectric loss for high-frequency signal transmission, *Front. Mater.*, 2021, **8**, 774843.
5 K. Maex, M. R. Baklanov, D. Shamiryan, F. lacopi, S. H. Brongersma and Z. S. Yanovitskaya, Low dielectric constant materials for microelectronics, *J. Appl. Phys.*, 2003, **93**, 8793–8841.
6 Z. Hu, X. Liu, T. Ren, H. A. M. Saeed, Q. Wang, X. Cui, K. Huai, S. Huang, Y. Xia, K. Fu, J. Zhang and Y. Chen, Research progress of low dielectric constant polymer materials, *J. Polym. Eng.*, 2022, **42**, 677–687.
7 W. Volksen, R. D. Miller and G. Dubois, Low dielectric constant materials, *Chem. Rev.*, 2010, **110**, 56–110.
8 J. Hou, L. Fang, G. Huang, M. Dai, F. Liu, C. Wang, M. Li, H. Zhang, J. Sun and Q. Fang, Low-dielectric polymers derived from biomass, *ACS Appl. Polym. Mater.*, 2021, **3**, 2835–2848.
9 L. Fang, J. Zhou, C. He, Y. Tao, C. Wang, M. Dai, H. Wang, J. Sun and Q. Fang, Understanding how intrinsic micropores affect the dielectric properties of polymers: An approach to synthesize ultra-low dielectric polymers with bulky tetrahedral units as cores, *Polym. Chem.*, 2020, **11**, 2674–2680.
10 Y. Wang, Y. Luo, K. Jin, J. Sun and Q. Fang, A spiro-centered thermopolymerizable fluorinated macromonomer: Synthesis and conversion to the high performance polymer, *RSC Adv.*, 2017, **7**, 18861–18866.
11 X. Huang, J. Wang, Q. Li, J. Lin and Z. Wang, Impact of the phenyl thioether contents on the high frequency dielectric loss characteristics of the modified polyimide films, *Surf. Coat. Technol.*, 2019, **360**, 205–212.
12 G. Maier, Low dielectric constant polymers for microelectronics, *Prog. Polym. Sci.*, 2001, **26**, 3–65.
13 Y. Cheng, W. Chen, Z. Li, T. Zhu, Z. Zhang and Y. Jin, Hydrolysis and condensation of a benzocyclobutene-functionalized precursor for the synthesis of high performance low-*k* polymers, *RSC Adv.*, 2017, **7**, 14406–14412.
14 R. A. Kirchhoff and K. J. Bruza, Benzocyclobutenes in polymer synthesis, *Prog. Polym. Sci.*, 1993, **18**, 85–185.
15 M. F. Farona, Benzocyclobutenes in polymer chemistry, *Prog. Polym. Sci.*, 1996, **21**, 505–555.
16 L. Kong, Y. Cheng, Y. Jin, Z. Ren, Y. Li and F. Xiao, Adamantyl-based benzocyclobutene low-*k* polymers with good physical properties and excellent planarity, *J. Mater. Chem. C*, 2015, **3**, 3364–3370.
17 L. Kong, T. Qi, Z. Ren, Y. Jin, Y. Li, Y. Cheng and F. Xiao, High-performance intrinsic low-*k* polymer via the synergistic effect of its three units: Adamantyl, perfluorocyclobutylidene and benzocyclobutene, *RSC Adv.*, 2016, **6**, 68560–68567.
18 S. F. Hahn, S. J. Martin and M. L. McKelvy, Thermally induced polymerization of an arylvinylbenzocyclobutene monomer, *Macromolecules*, 1992, **25**, 1539–1545.
19 F. Liu, J. Sun and Q. Fang, Biobased low-*k* polymers at high frequency derived from isoeugenol, *ACS Appl. Polym. Mater.*, 2022, **4**, 7173–7181.
20 F. Liu, J. Sun and Q. Fang, Fluorinated benzocyclobutene-based low-*k* polymer at high frequency, *ACS Appl. Polym. Mater.*, 2022, **4**, 842–848.
21 F. Fu, D. Wang, M. Shen, S. Shang, Z. Song and J. Song, Biorenewable rosin derived benzocyclobutene resin: A thermosetting material with good hydrophobicity and low dielectric constant, *RSC Adv.*, 2019, **9**, 29788–29795.
22 J. Hou, J. Sun and Q. Fang, A fluorinated low dielectric polymer at high frequency derived from allylphenol and benzocyclobutene by a facile route, *Eur. Polym. J.*, 2022, **163**, 110943.
23 Y. Wang, J. Zhou, J. Hou, X. Chen, J. Sun and Q. Fang, High-performance polyimides with high T_g and excellent dimensional stability at high temperature prepared via a cooperative action of hydrogen-bond interaction and cross-linking reaction, *ACS Appl. Polym. Mater.*, 2019, **1**, 2099–2107.
24 X. Yan, F. Dai, Z. Ke, K. Yan, C. Chen, G. Qian and H. Li, Synthesis of colorless polyimides with high T_g from asymmetric twisted benzimidazole diamines, *Eur. Polym. J.*, 2022, **164**, 110975.
25 D. W. Smith, D. A. Babb, R. V. Snelgrove, P. H. Townsend and S. J. Martin, Polynaphthalene networks from bisphenols, *J. Am. Chem. Soc.*, 1998, **120**, 9078–9079.
26 D. Mathew, C. P. Reghunadhan Nair and K. N. Ninan, Bisphenol A Dicyanate–Novolac epoxy blend: Cure characteristicsphysical and mechanical properties, and application in composites, *J. Appl. Polym. Sci.*, 1999, **74**, 1675–1685.

Open Access Article. Published on 20 June 2023. Downloaded on 4/6/2026 2:06:47 PM.
This article is licensed under a Creative Commons Attribution-NonCommercial 3.0 Unported Licence.

27 M. Dai, Y. Tao, L. Fang, C. Wang, J. Sun and Q. Fang, Low dielectric polymers with high thermostability derived from biobased vanillin, *ACS Sustainable Chem. Eng.*, 2020, **8**, 15013–15019.
28 G. Huang, J. Sun and Q. Fang, Thermo-crosslinkable molecular glasses towards the low *k* materials at high frequency, *Mater. Today Chem.*, 2022, **24**, 100782.
29 Q. Long, X. Li, Y. Huang, Q. Peng, X. Li, L. Zhu, J. Ma, X. Ye and J. Yang, The low dielectric constant hyperbranched polycarbosilane derived resins with spacing groups, *J. Appl. Polym. Sci.*, 2022, **139**, 52614.
30 S. Prasertsri and N. Rattanasom, Fumed and precipitated silica reinforced natural rubber composites prepared from latex system: Mechanical and dynamic properties, *Polym. Test.*, 2012, **31**, 593–605.
31 F. Fu, M. Shen, D. Wang, H. Liu, S. Shang, F.-L. Hu, Z. Song and J. Song, Facile strategy for preparing a rosin-based low-*k* material: Molecular design of free volume, *Biomacromolecules*, 2022, **23**, 2856–2866.
32 G. Huang, L. Fang, C. Wang, M. Dai, J. Sun and Q. Fang, A bio-based low dielectric material at a high frequency derived from resveratrol, *Polym. Chem.*, 2021, **12**, 402–407.
33 F. Liu, X. Chen, J. Hou, J. Sun and Q. Fang, A fluorinated thermocrosslinkable organosiloxane: A new low-*k* material at high frequency with low water uptake, *Macromol. Rapid. Commun.*, 2021, **42**, 2000600.
34 X. Chen, J. Sun, L. Fang, Y. Tao, X. Chen, J. Zhou and Q. Fang, Cross-linkable fluorinated polynorbornene with high thermostability and low dielectric constant at high frequency, *ACS Appl. Polym. Mater.*, 2019, **2**, 768–774.
35 L. Fang, Y. Tao, C. Wang, M. Dai, G. Huang, J. Sun and Q. Fang, Resveratrol-based fluorinated materials with high thermostability and good dielectric properties at high frequency, *ACS Sustainable Chem. Eng.*, 2020, **8**, 16905–16911.
36 Y. Luo, K. Jin, C. He, J. Wang, J. Sun, F. He, J. Zhou, Y. Wang and Q. Fang, An intrinsically microporous network polymer with good dielectric properties at high frequency, *Macromolecules*, 2016, **49**, 7314–7321.
37 J. Wang, J. Sun, J. Zhou, K. Jin and Q. Fang, Fluorinated and thermo-cross-linked polyhedral oligomeric silsesquioxanes: New organic–inorganic hybrid materials for high-performance dielectric application, *ACS Appl. Mater. Interfaces*, 2017, **9**, 12782–12790.
38 M. Dai, J. Sun and Q. Fang, A fluorinated cross-linked polystyrene with good dielectric properties at high frequency derived from bio-based vanillin, *Polym. Chem.*, 2022, **13**, 4484–4489.
39 F. Liu, X. Chen, L. Fang, J. Sun and Q. Fang, An effective strategy for the preparation of intrinsic low-*k* and ultralow-loss dielectric polysiloxanes at high frequency by introducing trifluoromethyl groups into the polymers, *Polym. Chem.*, 2020, **11**, 6163–6170.
40 Z. Feng, M. Zeng, D. Meng, J. Chen, W. Zhu, Q. Xu and J. Wang, A novel bio-based benzoxazine resin with outstanding thermal and superhigh-frequency dielectric properties, *J. Mater. Sci.: Mater. Electron.*, 2020, **31**, 4364–4376.

This journal is © The Royal Society of Chemistry 2023